Pulmonary Mastocytosis and Enhanced Lung Inflammation in Mice Heterozygous Null for the Foxf1 Gene

Tanya V. Kalin[1], Lucille Meliton[2], Angelo Y. Meliton[2], Xiangdong Zhu[2], Jeffrey A. Whitsett[1], and Vladimir V. Kalinichenko[1]

[1]Division of Pulmonary Biology, Cincinnati Children's Hospital Research Foundation, Cincinnati, Ohio; and [2]Department of Medicine, University of Chicago, Chicago, Illinois

The Forkhead Box f1 (Foxf1) transcriptional factor (previously known as HFH-8 or Freac-1) is expressed in endothelial and smooth muscle cells in the embryonic and adult lung. To assess effects of Foxf1 during lung injury, we used CCl_4 and butylated hydroxytoluene (BHT) injury models. *Foxf1*$^{+/-}$ mice developed severe airway obstruction and bronchial edema, associated with increased numbers of pulmonary mast cells and increased mast cell degranulation after injury. Pulmonary inflammation in *Foxf1*$^{+/-}$ mice was associated with diminished expression of Foxf1, increased mast cell tryptase, and increased expression of CXCL12, the latter being essential for mast cell migration and chemotaxis. After ovalbumin (OVA) sensitization and OVA challenge, increased lung inflammation, airway hyperresponsiveness to methacholine, and elevated expression of CXCL12 were observed in *Foxf1*$^{+/-}$ mice. During lung development, *Foxf1*$^{+/-}$ embryos displayed a marked increase in pulmonary mast cells before birth, and this was associated with increased CXCL12 levels in the lung. Expression of a doxycycline-inducible Foxf1 dominant-negative transgene in primary cultures of lung endothelial cells increased CXCL12 expression *in vitro*. Foxf1 haploinsufficiency caused pulmonary mastocytosis and enhanced pulmonary inflammation after chemically induced or allergen-mediated lung injury, indicating an important role for Foxf1 in the pathogenesis of pulmonary inflammatory responses.

Keywords: Foxf1; CXCL12; SDF-1; mast cells; lung injury

CLINICAL RELEVANCE

Foxf1 haploinsufficiency caused pulmonary mastocytosis and enhanced pulmonary inflammation after chemically induced or allergen-mediated lung injury, indicating an important role for Foxf1 in the pathogenesis of pulmonary inflammatory responses.

Mast cells are highly specialized cells that play important roles in adaptive and innate immunity, immunoglobulin E–mediated allergy, and inflammatory responses in the lung (1, 2). Immediately after exposure to allergens, mast cells release a variety of inflammatory mediators, including histamine, heparin, prostaglandins, and mast cell proteases, causing airway constriction, blood vessel dilatation and permeation, tissue swelling, hyperoxia, and eosinophil infiltration, contributing to pathogenesis of bronchial asthma (1, 2). Mast cells store tumor necrosis factor (TNF) and are thus primed to trigger TNF-mediated inflammatory responses (3). Mast cells also produce IL-4, IL-6, and IL-8, which play important roles in acute and chronic lung inflammation (2, 4). Mast cell recruitment is mediated by various factors, including platelet-derived growth factor (PDGF), vascular endothelial growth factor (VEGF), basic fibroblast growth factor (bFGF), transforming growth factor β (TGF-β), and stromal cell–derived factor-1 (SDF-1 or CXCL12) (4–6). CXCL12 is produced by fibroblasts and endothelial cells and binds to its receptor, CXCR4, present on the surface of mast cells. CXCL12 stimulates mast cell migration and IL-8 production (4, 7). Interestingly, activated mast cells are found in excessive numbers in tissues in heterogeneous clinical disorders associated with mastocytosis (8). Although a subset of patients with mastocytosis displayed activating mutations in *c-KIT* gene, little is known about transcriptional and signaling pathways contributing to molecular pathogenesis of this disease (8).

The Forkhead Box (Fox) family of transcription factors shares homology in the winged helix DNA-binding domain (9) and its members play important roles in cellular proliferation, differentiation, and metabolic homeostasis (10, 11). Forkhead Box f1 (Foxf1) is expressed in capillary endothelial cells, fibroblasts, and peribronchial smooth muscle cells of the embryonic and adult lung and other organs (12, 13). We and others have previously generated mice with targeted disruption of the *Foxf1* gene and demonstrated that *Foxf1*$^{-/-}$ embryos die by 8.5 days *post coitum* (dpc) due to defective vasculogenesis in the yolk sac and allantois (13, 14). Haploinsufficiency of the *Foxf1* gene in *Foxf1*$^{+/-}$ mice causes perinatal pulmonary hemorrhage, and severe defects in alveolarization and vascularization, as well as fusion of lung lobes and arteries (13, 15, 16). Perinatal lethality from pulmonary hemorrhage was observed in half of newborn *Foxf1*$^{+/-}$ mice that displayed the most severe reduction in pulmonary Foxf1 levels (13). Interestingly, the other half of the newborn *Foxf1*$^{+/-}$ mice displayed compensatory increases of Foxf1 mRNA levels in the lung, exhibited diminished alveolar septation without pulmonary hemorrhage, and survived postnatally (13). Adult *Foxf1*$^{+/-}$ mice had normal life spans and exhibited normal lung morphology in adulthood, suggesting that these mice compensated for the alveolar septation defect (17). However, in response to butylated hydroxytoluene (BHT)-mediated lung injury, the *Foxf1*$^{+/-}$ mice exhibited severe defects in lung repair and died from pulmonary hemorrhage (17).

Our previous studies demonstrated that Foxf1 is expressed in hepatic stellate and endothelial cells (18, 19). After carbon tetrachloride (CCl_4) injury, *Foxf1*$^{+/-}$ livers exhibited diminished activation of the hepatic stellate cells, associated with a significant reduction in α-smooth muscle actin, type I collagen, notch-2, and IP-10 proteins, indicating an important role for Foxf1 in liver repair and function (18).

(*Received in original form January 23, 2008 and in final form April 16, 2008*)

This work was supported by American Heart Association Grant 0335036N (to V.V.K.), Research Grant 6-FY2005–325 from the March of Dimes Birth Defects Foundation (to V.V.K.), and US Public Health Service Grant HL 84151 (to V. V. K.).

Correspondence and requests for reprints should be addressed to Vladimir V. Kalinichenko, Division of Pulmonary Biology, Cincinnati Children's Hospital Research Foundation, 3333 Burnet Ave., MLC 7009, Cincinnati, OH 45229. E-mail: Vladimir.Kalinichenko@cchmc.org

Originally Published in Press as DOI: 10.1165/rcmb.2008-0044OC on April 17, 2008
Internet address: www.atsjournals.org

In this article, we have demonstrated increased numbers of pulmonary mast cells and susceptibility of *Foxf1*$^{+/-}$ mice to pulmonary injury and inflammation. Increased numbers of pulmonary mast cells, increased mast cell degranulation, and bronchial edema caused airway obstruction in CCl_4-treated *Foxf1*$^{+/-}$ mice. Increased pulmonary inflammation in *Foxf1*$^{+/-}$ mice was associated with increased pulmonary expression of mast cell tryptase and CXCL12, the latter of which is essential for mast cell migration and chemotaxis. After ovalbumin (OVA) sensitization and OVA challenge, *Foxf1*$^{+/-}$ mice displayed increased lung inflammation, airway hyperresponsiveness to methacholine, and elevated expression of tryptase and CXCL12. Furthermore, increased numbers of mast cells and elevated CXCL12 levels were found in lungs of *Foxf1*$^{+/-}$ embryos, suggesting that Foxf1 haploinsufficiency causes a genetic predisposition to inflammatory lung diseases. Finally, using primary endothelial cells containing a doxycycline-inducible Foxf1 dominant-negative transgene, we demonstrated that Foxf1 deficiency increased CXCL12 expression *in vitro*. Foxf1 haploinsufficiency caused abnormal accumulation of mast cells during lung development and lung injury, contributing to genetic predisposition to chemically induced and antigen-mediated lung inflammation.

MATERIALS AND METHODS

Foxf1$^{+/-}$ Mice

Foxf1$^{+/-}$ mice in which the *Foxf1* allele was disrupted by an in-frame insertion of a nuclear localizing β-galactosidase (β-Gal) gene were bred for 10 generations into the Black Swiss mouse genetic background (13). Carbon tetrachloride (CCl_4; Sigma, St. Louis, MO) was dissolved in mineral oil at a 1:20 ratio vol/vol, and a single intraperitoneal injection of CCl_4 (0.5 μl of CCl_4/1 g of body weight) was administered to male *Foxf1*$^{+/-}$ mice or their wild-type (WT) littermates as described (18, 20). In separate experiments, *Foxf1*$^{+/-}$ and WT mice were injected intraperitoneally with BHT (300 mg/kg body weight) to induce lung injury as described (12, 17, 21). To determine statistical significance of any observed differences, we used five *Foxf1*$^{+/-}$ and WT mice in each group. Mice were killed by CO_2 asphyxiation, and the left lung lobe was used to prepare total RNA. Right lung lobes were fixed overnight in 4% paraformaldehyde (PFA) at 4°C and then paraffin embedded.

Immunization and Airway Challenge with OVA

Foxf1$^{+/-}$ and WT mice were immunized with 10 μg of OVA mixed with 1.125 mg of aluminum hydroxide (Imgect Alum; Pierce Chemical Co., Rockford, IL) on Days 0, 7, and 14 as described previously (22). On Days 21 to 24, mice were exposed to aerosolized OVA (1%) or saline for 40 minutes (22). Twenty-four hours after the last OVA challenge, mice were killed, and the mouse lungs were used for paraffin embedding or preparation of total lung RNA.

Collection and Analysis of Bronchoalveolar Lavage Fluid

Bronchoalveolar lavage (BAL) fluid was collected either 24 hours after the final dose of OVA or 18 hours after CCl_4 treatment. BAL was performed by delivering 0.8 ml cold PBS into the airway through a trachea cannula and gently aspirating the fluid. The lavage was repeated three times to recover a total volume of 2 to 3 ml. The cells were stained with Trypan blue to determine viability and with Turk solution to obtain total nucleated cell counts using a hemocytometer. Cytospin (Cytospin 2; Shandon, Waltham, MA) slides were prepared from the BAL fluid and were then fixed and stained using Diff-Quick reagent (Dade Diagnostics, Deerfield, IL). Differential cell counts were determined by counting 300 cells per each slide using standard morphologic criteria in a single-blind method. Five mice were used for each group.

Measurement of Cytokine Levels

The concentrations of IL-4, IL-5, and IFN-γ in BAL fluid were measured using a Mouse Cytokine CBA kit (BD Biosciences, San Diego, CA) according to the manufacturer's recommendations. The concentrations of CXCL12 in BAL fluid and serum was determined by a quantitative immunoassay from R&D Systems (Minneapolis, MN).

Measurements of Airway Responsiveness to Methacholine

Methacholine challenge was performed either 24 hours after the final dose of OVA or 18 hours after CCl_4-treatment. Pulmonary function testing was performed using a computer-controlled small-animal ventilator (SAV) (Flexivent; Scireq, Montreal, PQ, Canada) as previously described (22). Briefly, mice were anesthetized with 30 mg/kg xylazine and 80 mg/kg ketamine intraperitoneally, and the trachea was cannulated with an 18-gauge metal needle connected to the SAV. Regular mechanical ventilation was applied, and animals were ventilated quasi-sinusoidally at a frequency of 120 breaths/minute at a tidal volume of 6 ml/kg. The expiratory valve of the SAV allowed the animal to empty passively through a water trap adjusted to maintain a positive end-expiratory pressure of 2.0 cm H_2O. This positive end-expiratory pressure was shown to be optimal for the determination of methacholine-induced changes in respiratory system resistance (22). Increasing doses of methacholine (1.25–20 mg/ml) were delivered at 5-minute intervals using inhalation method.

Immunohistochemical Staining

Sections of paraffin-embedded lung tissue were stained with hematoxylin and eosin or used for immunohistochemical staining with mouse monoclonal antibodies against mast cell tryptase (clone AA1; Lab Vision, Fremont, CA). Antibody–antigen complexes were detected using anti-mouse antibody conjugated with alkaline phosphatase (AP) and BCIP/NBT substrate (all from Vector Labs, Burlingame, CA) as described (12). Lung sections were counterstained with nuclear fast red (Vector Labs).

RNase Protection Assay

Total mouse RNA was prepared by an acid guanidium-thiocyanate-phenol-chloroform extraction method using RNA-STAT-60 (Tel-Test "B" Inc., Friendswood, TX) from mouse lungs or primary lung endothelial cells. Primers specific for mouse tryptase (5′-gccaatgacacctactg gatgc-3′ and 5′-gggtttgtgagtttcagcaggg-3′) were used to amplify tryptase cDNA fragment from total lung RNA and then clone it into the pCRII plasmid to synthesize antisense RNA probes. RNase protection assay was performed with [^{32}P] UTP-labeled antisense RNA synthesized from mouse tryptase cDNA as described previously (23). RNA probe hybridization, RNase One (Promega, Madison, WI) digestion, electrophoresis of RNA protected fragments, and autoradiography were performed as described previously (13). Gene expression levels were determined by analysis of phosphorimager scans using the ImageQuant program (Amersham Biosciences, Inc., Piscataway, NJ) as described previously (24, 25). Hybridization signals for mouse cyclophilin and ribosomal L32 protein mRNAs were used for normalization.

Analysis of Applied Biosystems Expression Arrays

Hybridization of the Applied Biosystems Mouse Genome Survey Microarray (P/N 4345065; Applied Biosystems, Framingham, MA) was performed using 2 μg of total lung RNA in the Functional Genomic Facility of the University of Chicago. For this assay, each sample contained a mixture of equal amounts of RNA from three distinct *Foxf1*$^{+/-}$ or WT mice, each treated with CCl_4 for 16 hours. Images were analyzed using the Applied Biosystems 1700 Chemiluminescent Microarray Analyzer software v 1.1.

Quantitative Real-Time RT-PCR

Total RNA was digested with RNAse-free DNase I to remove contaminating genomic DNA, and then purified using the Qiagen RNeasy Micro Kit (Cat. # 74004; Qiagen, Germantown, MD). We used the Bio-Rad cDNA Synthesis Kit (Bio-Rad, Hercules, CA) containing both oligo-dT and random hexamer primers to synthesize cDNA from 10 μg of total RNA as described (26). Quantitative RT-PCR primers for mouse cyclophilin were described previously (26). The following sense and anti-sense primers were used for amplification: mast cell tryptase, 5′-caccctgtccccctacct-3′ and 5′-atgtccttcattcccagcac-3′; Foxf1, 5′-cct ggagcagccatacctt-3′ and 5′-taagatcctccgcctgttgt-3′; CXCL12, 5′-ctcctgta gaatggagccaga-3′ and 5′-ttcgatcagagcccatagag-3′; endomucin, 5′-caac tacggcatgttttcca-3′ and 5′-gaggaaccaacacaatttcca-3′; mast cell protease -5,

5′-ttcatctgctgctccttctcctgg-3′ and 5′-ggctttctccttcaacttcagtagc-3′. Mouse cyclophilin was used for normalization control as described previously (25).

Cotransfection Studies and Infection of Primary Endothelial Cells with Recombinant Adenoviruses

Endothelial cells (ECs) were isolated from 10-d-old WT and transgenic TetO-Foxf1 DN mice using a tissue digestion, binding with endothelial-specific Pecam-1 antibodies followed by EC purification using immunomagnetic beads as described (27, 28). The purity of pulmonary ECs was 95.1 ± 2.7%, as demonstrated by cytochemical staining with fluorescein isothiocyanate (FITC)-conjugated isolectin B4, a specific marker of endothelial cells (13).

The TetO-Foxf1 dominant-negative (DN) transgene contains the CMV-Tet operator (TetO) promoter, which drives the expression of a T7-tagged Foxf1 DNA binding domain fused to *engrailed* transcriptional repression domain (29). Cultured ECs were transiently transfected with 6× Foxf1-TATA-luciferase (LUC) reporter construct (30) and CMV-Foxf1 expression plasmid using Fugene 6 reagent (Roche, Indianapolis, IN) as described previously (29, 30). A CMV-Renilla construct was used as an internal control to normalize transfection efficiency. Two hours after transfection, ECs were infected at a multiplicity of infection (MOI) of 100 ifu per cell with adenovirus containing Tetracycline activator (Ad-TA, Tet-off system) or with control LacZ adenovirus (Ad-LacZ) as described (19, 29). Dual luciferase assays (Promega) were performed 48 h after the adenoviral infection as described previously (19, 30). In separate experiments, WT and transgenic ECs were infected with either Ad-TA or Ad-LacZ and then used for preparation of total RNA or for immunofluorescent staining. ECs were fixed with 10% paraformaldehyde and then stained with mouse monoclonal antibodies against T7 followed by anti-mouse antibody conjugated with TRITC as described (29).

Statistical Analysis

The Student's *t* test was used to determine statistical significance. *P* values less than 0.05 were considered significant. Values for all measurements were expressed as the mean ± SD.

RESULTS

CCl_4 Treatment Causes Bronchial Obstruction in *Foxf1*$^{+/-}$ Mice

To assess whether Foxf1 insufficiency influenced lung injury, we used CCl_4 and BHT injury models. In studies of CCl_4 toxicity in

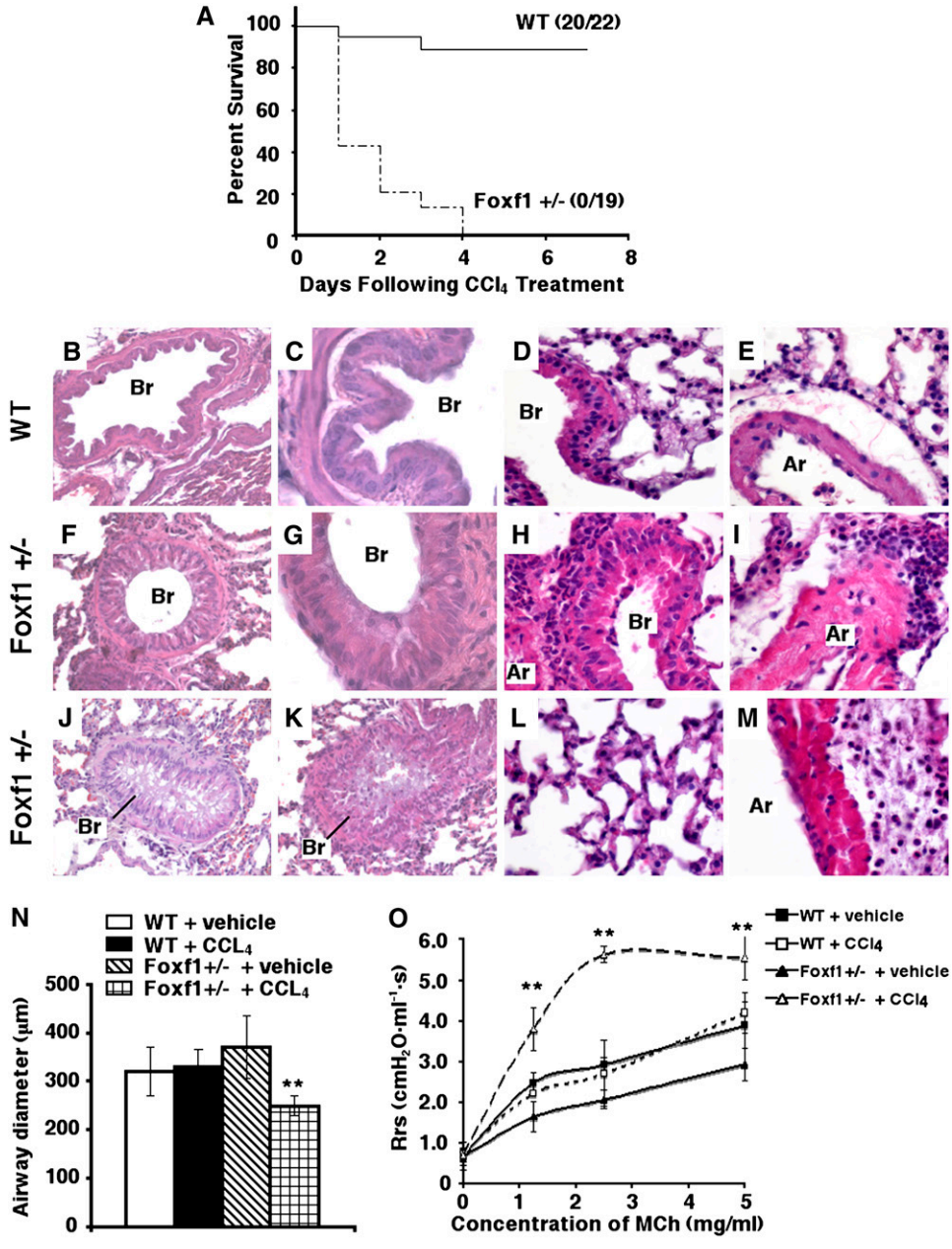

Figure 1. Lung inflammation, airway obstruction, and mortality in *Foxf1*$^{+/-}$ mice after CCl_4 injury. (*A*) CCl_4 treatment causes mortality in *Foxf1*$^{+/-}$ mice. Graphic representation of percent survival of wild-type (WT) and *Foxf1*$^{+/-}$ mice after CCl_4 injury. WT and *Foxf1*$^{+/-}$ mice were injected with CCl_4 and percentage of survival at different intervals after CCl_4 injury was calculated. (*B–M*) CCl_4 injury induces lung inflammation in *Foxf1*$^{+/-}$ mice. Paraffin sections were prepared from lungs of either WT or *Foxf1*$^{+/-}$ mice 18 hours after CCl_4 injection. Hematoxylin and eosin staining (H&E) shows severe narrowing of large airways in CCl_4-treated *Foxf1*$^{+/-}$ mice (*F–H*), as well as airway obstruction (*J* and *K*), leukocyte infiltration (*H–I, M*) and accumulation of fluid occluding the airway lumen in *Foxf1*$^{+/-}$ lungs (*J* and *K*). Leukocyte infiltration is not observed in alveolar regions of in CCl_4-treated *Foxf1*$^{+/-}$ mice (*L*). No lung injury or lung inflammation is detected in CCl_4-treated WT mice (*B–E*). (*N*) Decreased airway diameter in CCl_4-treated *Foxf1*$^{+/-}$ mice. H&E-stained sections were used to measure the diameter of bronchioles in WT or *Foxf1*$^{+/-}$ mice 18 hours after CCl_4 injection. Mice injected with vehicle (mineral oil) were used as controls. Mean ± S.D. was calculated using twenty bronchioles in each lung. Five mice were used in each group. *Asterisks* indicate statistically significant differences with *P* values < 0.05 as calculated by Student's *t* test. (*O*) CCl_4-treated *Foxf1*$^{+/-}$ mice displayed increased airway responsiveness to methacholine. Airway responsiveness was measured 18 hours after CCl_4 injection. CCl_4 treatment increased airway responsiveness to 1.25–5 mg/ml of methacholine in *Foxf1*$^{+/-}$ mice (*open triangles*) when compared with either CCl_4-treated WT mice (*open squares*) or vehicle-treated *Foxf1*$^{+/-}$ (*solid triangles*) and WT mice (*solid squares*). Ar, artery; Br, bronchiole. *Magnification*: *B, F, J,* and *K,* ×200; *D, E, H, I, L,* and *M,* ×400; *C* and *G,* ×680.

Foxf1$^{+/-}$ mice, approximately 60% of the *Foxf1*$^{+/-}$ mice died within the initial 24 hours after CCl_4 treatment (Figure 1A). While CCl_4 is hepatotoxic, serum levels of liver aminotransferases, alkaline phosphatase, bilirubin, and albumin were similar in CCl_4-treated *Foxf1*$^{+/-}$ and WT mice (data not shown), indicating that the increased mortality of *Foxf1*$^{+/-}$ mice during the initial 24 hours of CCl_4 treatment did not result from liver failure. Since Foxf1 is essential for formation of pulmonary capillaries (13), we considered the possibility that capillary insufficiency and lung hemorrhage associated with partial loss of Foxf1 function may contribute to the observed increased early mortality in *Foxf1*$^{+/-}$ mice. However, at the light microscopic level, no detectable changes were observed in the vascular bed of CCl_4-treated *Foxf1*$^{+/-}$ lungs compared with WT lungs (data not shown).

In contrast to WT mice, CCl_4-treated *Foxf1*$^{+/-}$ lungs displayed severe narrowing of large airways (Figures 1B-1I), leading to airway occlusion (Figures 1J and 1K). The average diameter of pulmonary bronchioles in CCl_4-treated *Foxf1*$^{+/-}$ mice was significantly decreased compared with pulmonary bronchioles in either WT mice or vehicle-treated *Foxf1*$^{+/-}$ mice (Figure 1N). Furthermore, the airway obstruction in CCl_4-treated *Foxf1*$^{+/-}$ mice was associated with increased airway resistance as demonstrated by airway responsiveness to methacholine (Figure 1O). These results suggested that CCl_4-induced bronchial obstruction contributed to the increased mortality of *Foxf1*$^{+/-}$ mice.

CCl_4 Treatment Causes Abnormal Lung Inflammation in *Foxf1*$^{+/-}$ Mice

In contrast to WT mice, CCl_4 treatment caused a leukocyte infiltration in *Foxf1*$^{+/-}$ lungs, which was mainly observed in interstitial tissue surrounding airways and pulmonary blood vessels (Figures 1D, 1E, 1H, and 1I). BAL fluid of CCl_4-treated *Foxf1*$^{+/-}$ mice contained increased numbers of eosinophils and macrophages when compared with BAL of either WT mice or vehicle-treated *Foxf1*$^{+/-}$ mice (Figure 2A). Lymphocyte and neutrophil numbers were unaltered in BAL of *Foxf1*$^{+/-}$ mice (Figure 2A). Increased inflammation in CCl_4-treated *Foxf1*$^{+/-}$ lungs was associated with increased concentrations of IL-4, IL-5, and IFN-γ proteins in BAL fluid (Figure 2B). These results demonstrated that CCl_4 treatment induced pulmonary inflammation, leukocyte infiltration, and cytokine production in *Foxf1*$^{+/-}$ lungs.

Increased Numbers of Mast Cells in *Foxf1*$^{+/-}$ Lungs

Morphologic examination of HE-stained lung sections and immunostaining with tryptase antibody revealed increased numbers of mast cells in CCl_4-treated *Foxf1*$^{+/-}$ lungs (Figures 3A–3F). Tryptase-positive mast cells were observed in alveolar, peribronchial, and perivascular regions (Figures 3G–3I). Increased tryptase immunoreactivity was also observed in the lumen of *Foxf1*$^{+/-}$ pulmonary airways (Figure 3F), a finding consistent with activation of mast cells (31, 32). Consistent with increased tryptase staining in CCl_4-injured *Foxf1*$^{+/-}$ lungs, tryptase mRNA levels were increased 7-fold (Figure 3J). Furthermore, numbers of tryptase-positive mast cells in liver, kidney, and intestine of CCl_4-treated *Foxf1*$^{+/-}$ mice remained unaltered (data not shown), indicating that the CCl_4-mediated inflammation was restricted to the *Foxf1*$^{+/-}$ lung. Thus, haploinsufficiency of the *Foxf1* gene caused bronchial obstruction and increased numbers of activated mast cells after $CC1_4$-induced injury, perhaps contributing to bronchial edema and mortality of CCl_4-treated *Foxf1*$^{+/-}$ mice. Interestingly, numbers of tryptase-positive mast cells were increased in lungs of *Foxf1*$^{+/-}$ mice before injury (Figure 3D). Mast cells were not detected in normal lung tissue from untreated WT mice (Figure 3A). Thus, Foxf1 influences mast cell accumulation in the lung that may in turn influence susceptibility to lung injury.

CCl_4 Treatment Causes Increased Expression of CXCL12 in the *Foxf1*$^{+/-}$ Lung

To identify genes influenced by Foxf1 during lung injury, we performed hybridization analysis of Applied Biosystems mouse expression arrays with cDNA probes generated from total lung RNA prepared from CCl_4-treated *Foxf1*$^{+/-}$ and CCl_4-treated WT mice (*see* GEO database for a complete list of genes with altered expression levels in CCl_4-treated *Foxf1*$^{+/-}$ lungs; www.ncbi.nim.nih.gov/geo; accession # GSE11112). This analysis revealed that CCl_4-treated *Foxf1*$^{+/-}$ lungs exhibited a 2.5-fold reduction in Foxf1 mRNA levels (data not shown), consistent with diminished Foxf1 expression during BHT-mediated lung injury (17). Expression of several inflammation-associated genes was increased in *Foxf1*$^{+/-}$ mice after CCl_4 treatment (data not shown), a finding consistent with increased inflammation in CCl_4-treated *Foxf1*$^{+/-}$ mice. The up-regulated genes included endomucin and stromal cell–derived factor 1 (SDF-1 or CXCL12), the

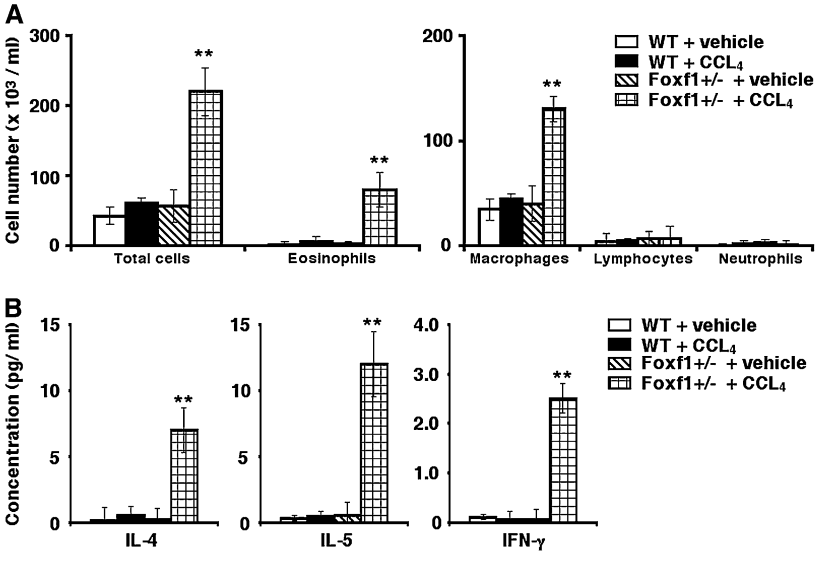

Figure 2. CCl_4 treatment causes increased airway inflammation in *Foxf1*$^{+/-}$ mice. (*A*) Increased leukocyte number in CCl_4-treated *Foxf1*$^{+/-}$ airways. Bronchoalveolar lavage (BAL) fluid was collected from WT or *Foxf1*$^{+/-}$ mice 18 hours after CCl_4 treatment. Mice treated with vehicle (mineral oil) were used as controls. CCl_4-treated *Foxf1*$^{+/-}$ mice displayed increased total cell count, which was largely composed of eosinophils and macrophages. Lymphocyte and neutrophil numbers were unaltered. Mean ± SD was calculated using five mice in each group. (*B*) CCl_4 treatment causes increased cytokine concentrations in BAL fluid of *Foxf1*$^{+/-}$ mice. CCl_4-treated *Foxf1*$^{+/-}$ lungs displayed increased concentrations of IL-4, IL-5, and IFN-γ proteins in BAL fluid. *Asterisks* indicate statistically significant differences with P values < 0.05 as calculated by Student's t test.

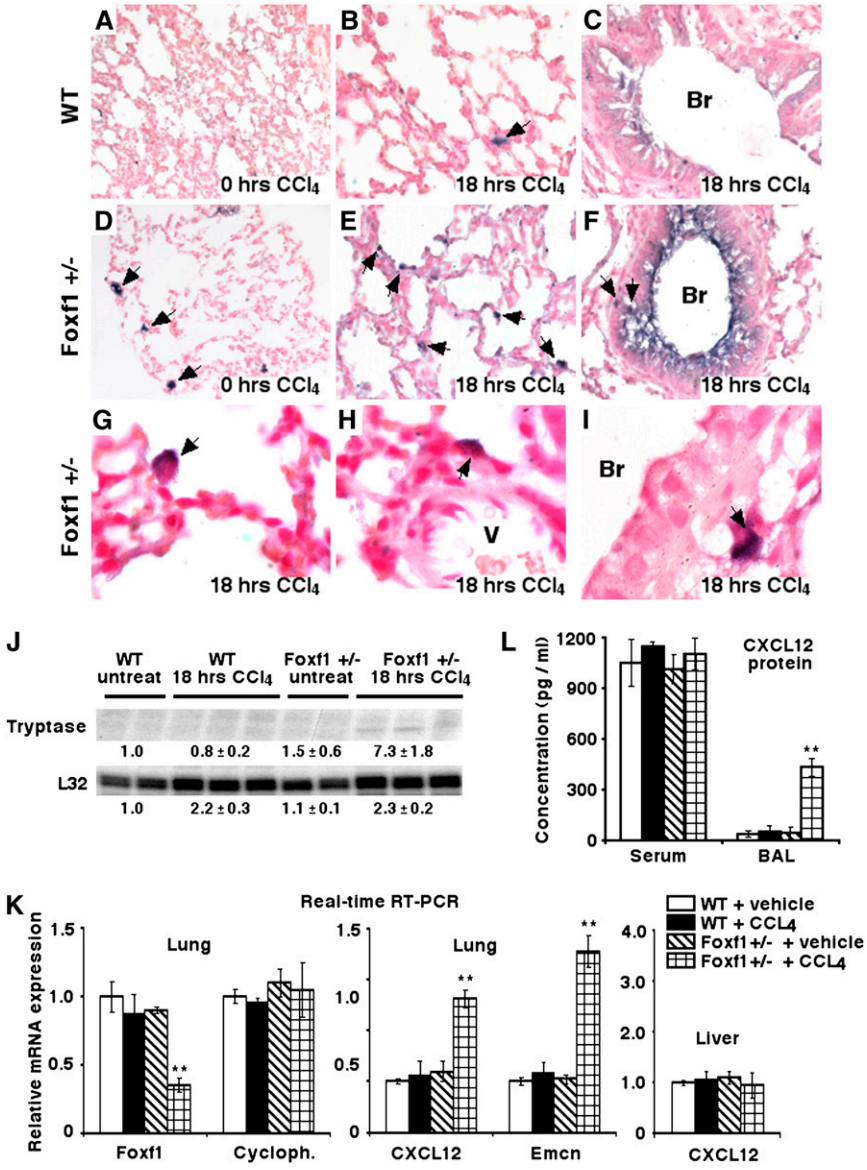

Figure 3. Pulmonary mastocytosis is associated with increased expression of mast cell tryptase and CXCL12 in *Foxf1*$^{+/-}$ lungs. (*A–I*) Increased numbers of mast cells in *Foxf1*$^{+/-}$ lungs. Paraffin lung sections from either untreated (0 h CCl_4) or CCl_4-treated WT and *Foxf1*$^{+/-}$ mice were stained with antibodies against mast cell tryptase (stains *dark violet*). Lung sections were counterstained with nuclear fast red (stains *red*). CCl_4 treatment caused increased numbers of tryptase-positive mast cells (shown with *arrows*) in alveolar (*E* and *G*), peribronchial (*F* and *I*) and perivascular regions (*H*) of *Foxf1*$^{+/-}$ lungs compared with WT lungs (*A–C*). Tryptase-positive mast cells were also detected in untreated *Foxf1*$^{+/-}$ lungs (*D*). CCl_4 injury caused an accumulation of tryptase in bronchial airspaces of *Foxf1*$^{+/-}$ lungs (*F*). *Magnification*: *A–F*, ×200; *G–I*, ×1,000. (*J*) CCl_4-treated *Foxf1*$^{+/-}$ lungs exhibited increased tryptase mRNA levels. Total lung RNA was isolated from either untreated or CCl_4-treated WT and *Foxf1*$^{+/-}$ mice and then analyzed for tryptase and ribosomal L32 by RNase protection assays. Each individual sample was normalized to its corresponding L32 level. Numbers represent means ± SD from three independent experiments. (*K*) Increased CXCL12 expression in CCl_4-treated *Foxf1*$^{+/-}$ lungs. Total RNA was prepared from left lung lobe of WT and *Foxf1*$^{+/-}$ mice treated with either CCl_4 or vehicle (mineral oil). Quantitative real-time RT-PCR was performed with primers specific to mouse Foxf1, CXCL12, endomucin (Emcn), and cyclophilin. Each individual sample was normalized to its corresponding cyclophilin level. (*L*) Increased concentrations of CXCL12 protein in BAL fluid of CCl_4-treated *Foxf1*$^{+/-}$ lungs. BAL fluid was collected from WT or *Foxf1*$^{+/-}$ mice after CCl_4 treatment. Five mice were used for each group. *Asterisks* indicate statistically significant differences with P values < 0.05.

latter of which is known to regulate mast cell migration and chemotaxis (4).

Quantitative real-time RT-PCR (qRT-PCR) analysis was used to confirm that the CCl_4-treated *Foxf1*$^{+/-}$ lungs exhibited diminished expression of Foxf1, whereas CXCL12 and endomucin mRNAs were increased in *Foxf1*$^{+/-}$ lungs (Figure 3K). Increased levels of CXCL12 protein were also found in BAL fluid of CCl_4-treated *Foxf1*$^{+/-}$ mice (Figure 3L). CXCL12 expression was not altered in the liver (Figure 3K) or blood serum of *Foxf1*$^{+/-}$ mice (Figure 3L). Furthermore, CXCL12 mRNA and protein levels were similar in vehicle-treated WT and *Foxf1*$^{+/-}$ lungs (Figures 3K and 3L), indicating that the CXCL12 expression was induced by CCl_4-mediated pulmonary inflammation.

BHT Injury Causes Increased Tryptase and CXCL12 Levels

To test whether lung injury responses were specific for CCl_4, we tested whether *Foxf1*$^{+/-}$ mice were susceptible to BHT-induced lung injury. BHT was given as a single intraperitoneal injection to *Foxf1*$^{+/-}$ and WT male mice (12, 17). Total lung RNA was prepared 2 or 6 days after BHT injection and used for qRT-PCR. After injury, consistent with previous studies (17), Foxf1 mRNA was decreased in BHT-injured *Foxf1*$^{+/-}$ lungs compared with control WT lungs (Figure 4). Increased pulmonary inflammation with bronchial edema and increased CXCL12 mRNA were observed after BHT exposure in *Foxf1*$^{+/-}$ mice (Figure 4) (17, and data not shown). Mast cell tryptase and endomucin expression were also increased in lungs of BHT-injured *Foxf1*$^{+/-}$ mice (Figure 4), indicating the presence of activated mast cells and elevated mucus production.

Persistent Pulmonary Inflammation and Airway Hyperresponsiveness in *Foxf1*$^{+/-}$ Mice after OVA-Mediated Lung Injury

Our studies demonstrated that haploinsufficiency of the *Foxf1* gene causes an increase in the number of pulmonary mast cells, and renders the mice sensitive to bronchial inflammation and airway obstruction after CCl_4 and BHT injury. Since increased numbers of mast cells were found in lungs of untreated *Foxf1*$^{+/-}$ mice, we considered that Foxf1 haploinsufficiency might contribute to antigen-mediated lung inflammation similar to that occurring in asthma. To test this, *Foxf1*$^{+/-}$ and WT mice were sensitized with three injections of OVA and then challenged with either aerosolized OVA or saline (22). Consistent with previous studies (22), OVA challenges induced inflammation in

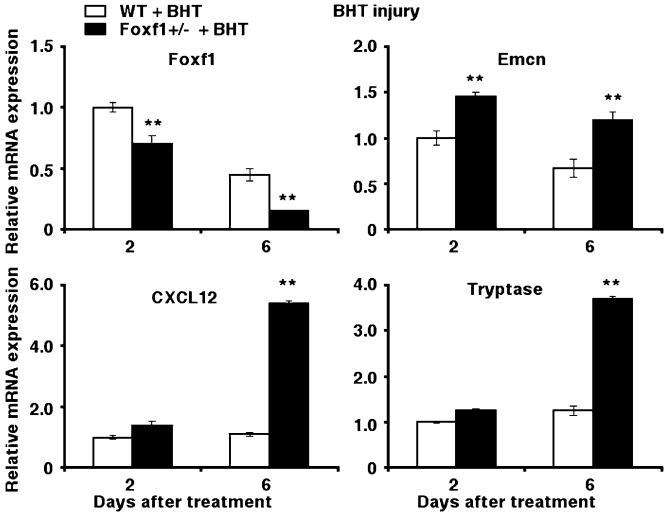

Figure 4. Increased CXCL12 expression in BHT-treated *Foxf1*$^{+/-}$ lungs. Total RNA was prepared from left lung lobe of WT and *Foxf1*$^{+/-}$ mice treated with BHT for 2 or 6 days. QRT-PCR was used to determine the expression levels of Foxf1, CXCL12, endomucin (Emcn), mast cell tryptase, and cyclophilin. Each individual sample was normalized to its corresponding cyclophilin level. *Asterisks* indicate statistically significant differences with $P < 0.05$.

interstitial tissue surrounding airways and pulmonary blood vessels in control and *Foxf1*$^{+/-}$ mice (Figure 5A). Inflammation was more severe in *Foxf1*$^{+/-}$ mice, as demonstrated by an increased number of inflammatory cells in the lung tissue (Figure 5A) and BAL fluid (Figure 5B). BAL fluid of OVA-treated *Foxf1*$^{+/-}$ mice contained a significant increase in numbers of eosinophils, whereas numbers of macrophages, lymphocytes, and neutrophils remained unaltered compared with OVA-treated WT mice (Figure 5B). OVA-treated *Foxf1*$^{+/-}$ mice also displayed increased concentrations of IL-4 and IL-5 proteins in BAL fluid compared with OVA-treated WT mice (Figure 5C). Consistent with the increased pulmonary inflammation in *Foxf1*$^{+/-}$ lungs, airway resistance during methacholine treatment was significantly increased (Figures 5D and 5E). Increased inflammation in *Foxf1*$^{+/-}$ lungs was associated with reduced Foxf1 mRNA and increased expression of mast cell tryptase (Figure 5G), as well as with increased CXCL12 mRNA (Figure 5G) and protein levels (Figure 5F). These results are consistent with BHT and CCl_4-mediated lung injury in *Foxf1*$^{+/-}$ mice. Taken together, these lung injury studies demonstrate that Foxf1 haploinsufficiency causes an increased susceptibility to either antigen-mediated or chemically-induced lung inflammation.

Increased Numbers of Pulmonary Mast Cells and Elevated CXCL12 Levels in *Foxf1*$^{+/-}$ Embryos

Next we determined whether increased CXCL12 expression and increased mast cell numbers occurred in *Foxf1*$^{+/-}$ embryonic lungs before birth. Paraffin lung sections from WT and *Foxf1*$^{+/-}$ E18.5 embryos were used for immunohistochemical staining with antibodies specific to mast cell protease 7 (tryptase), a known marker for mast cells (33). Although tryptase staining was not detected in WT lungs, increased numbers of tryptase-positive mast cells were observed in lungs from *Foxf1*$^{+/-}$ embryos at E18.5 (Figure 6C). Likewise, tryptase and mast cell–specific protease 5 mRNAs were increased in RNase protection assays (Figure 6A) and RT-PCR analysis (Figure 6B), confirming increased numbers of mast cells in *Foxf1*$^{+/-}$ lungs. Increased tryptase was observed in *Foxf1*$^{+/-}$ mice as early as E15.5 (Figure 6A). Furthermore, CXCL12 mRNA was increased in lungs from *Foxf1*$^{+/-}$ embryos at E15.5 and E18.5 (Figure 6D) and was correlated with elevated tryptase expression (Figure 6A) and increased numbers of pulmonary mast cells (Figure 6C). Since CXCL12 is essential for migration of mast cells into lung tissue (4), our results suggest that increased CXCL12 expression may contribute to the accumulation of mast cells seen in *Foxf1*$^{+/-}$ embryonic lungs. Interestingly, accumulation of mast cells was specific for *Foxf1*$^{+/-}$ lung tissue because normal mast cell numbers and tryptase mRNA levels were observed in embryonic *Foxf1*$^{+/-}$ livers and intestine (data not shown). These results suggest that Foxf1 haploinsufficiency causes pulmonary mastocytosis and increased CXCL12 expression during lung development.

Foxf1 Regulates CXCL12 Expression *In Vitro*

The Foxf1 transcription factor is not expressed in pulmonary mast cells or their precursors (18, 34), but is co-expressed with CXCL12 in pulmonary endothelial cells (18, 34), supporting the concept that pulmonary mastocytosis is related to migration/ engraftment of mast cell precursors into the lung rather then changes in differentiation or growth of hematopoetic precursors *per se*. To determine whether Foxf1 directly affects CXCL12 expression in endothelial cells, we used primary lung ECs prepared from either WT or TetO-Foxf1 DN transgenic mice. The TetO-Foxf1 DN mouse line uses the CMV-Tet operator (TetO) promoter to drive expression of a T7-tagged Foxf1 dominant-negative (Foxf1 DN) fusion protein (29). Purity of pulmonary ECs was 95.1 ± 2.7%, as demonstrated by cytochemical staining with FITC-conjugated isolectin B4 (Figures 7A and 7B), a specific marker of endothelial cells (13).

To activate the TetO-Foxf1 DN transgene in cell culture, transgenic ECs were infected for 48 hours with either CMV-Tetracycline activator adenovirus (Ad-TA) or LacZ control adenovirus (AdLacZ). Immunofluorescent staining with T7 antibody demonstrated that the Foxf1 DN protein was induced by Ad-TA infection (Tet-off system) in transgenic TetO-Foxf1 DN ECs, but was not in Ad-TA–infected wild type ECs (Figure 7E) or in transgenic TetO-Foxf1 DN ECs infected with AdLacZ adenovirus (Figure 7D). Cotransfection studies with the CMV-Foxf1 expression vector and the 6× Foxf1-TATA-luciferase reporter plasmid showed that Foxf1 DN protein inhibited Foxf1 transcriptional activity in transgenic TetO-Foxf1 DN ECs when they were infected with Ad-TA adenovirus (Figure 7G). In contrast, both AdLacZ-infected transgenic ECs and Ad-TA–infected WT ECs displayed normal Foxf1 transcriptional activity compared with uninfected ECs (Figure 7G). Thus, conditional expression of the Foxf1 DN transgene in ECs reduced the Foxf1 transcriptional activity. Decreased Foxf1 activity in TetO-Foxf1 DN ECs was associated with increased CXCL12 mRNA as demonstrated by qRT-PCR (Figure 7H). Thus CXCL12 expression is enhanced by inhibition of Foxf1 in cultured pulmonary endothelial cells.

DISCUSSION

Foxf1 is an important transcriptional regulator expressed in the developing mesenchyme and its derivatives: fibroblasts, endothelial cells, and smooth muscle cells (13, 14, 18). Although previous studies demonstrated that Foxf1 was critical for vascular integrity during lung development and lung injury (13, 17), molecular mechanisms underlying the Foxf1 function in the lung remain largely unknown. In this study, we demonstrated that lungs of *Foxf1*$^{+/-}$ embryos exhibited increased numbers of mast cells and increased expression of tryptase, mast cell protease-5, and CXCL12 chemokine, the latter of which is known to promote

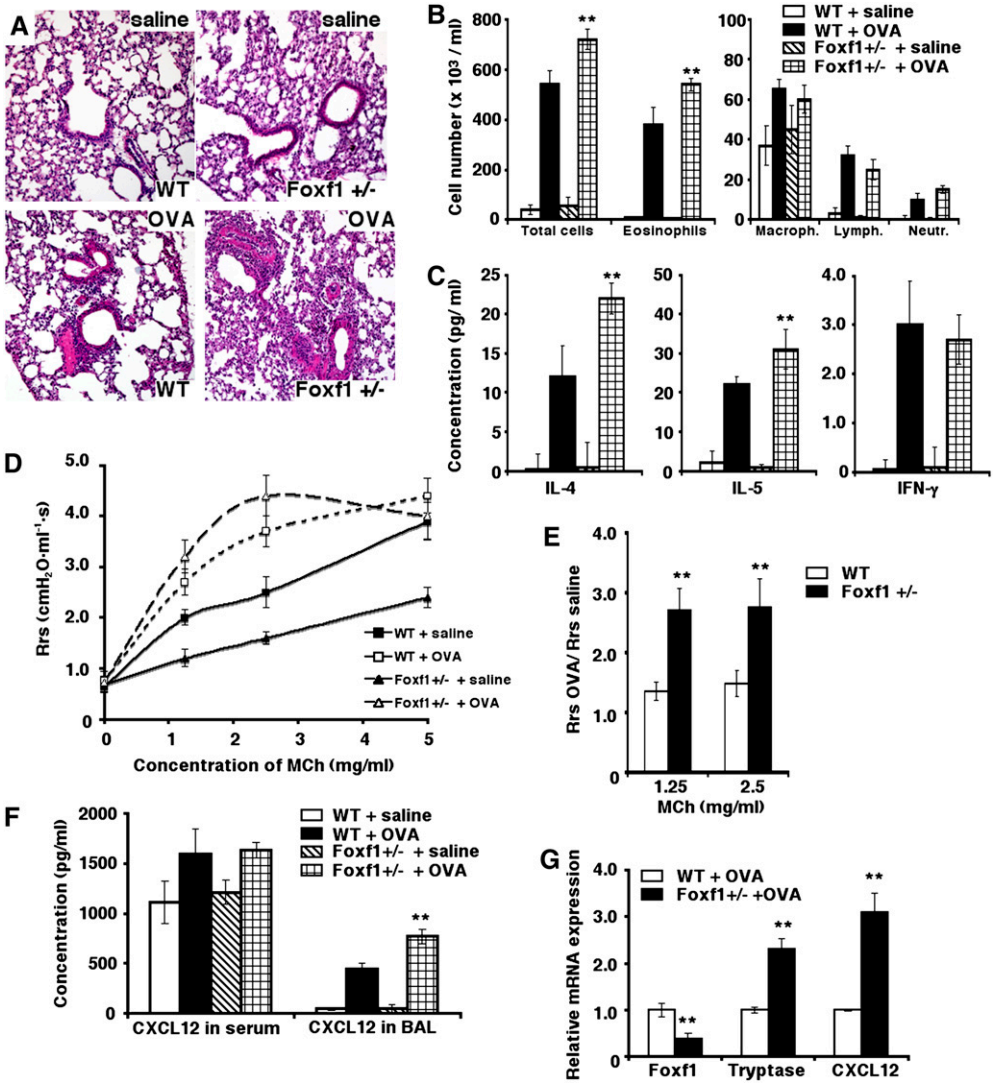

Figure 5. Increased pulmonary inflammation, airway hyperresponsiveness and increased CXCL12 expression following OVA-mediated lung injury in *Foxf1*$^{+/-}$ mice. (*A*) Increased inflammation in OVA-challenged *Foxf1*$^{+/-}$ lungs. WT and *Foxf1*$^{+/-}$ mice were immunized with OVA and then subjected to four OVA challenges on Days 21, 22, 23, and 24. Mice challenged with saline were used as controls. Paraffin lung sections were stained with H&E. *Magnification*: ×100. (*B* and *C*) OVA treatment causes increased leukocyte numbers and cytokine concentration in *Foxf1*$^{+/-}$ airways. BAL fluid was collected from WT or *Foxf1*$^{+/-}$ mice 24 hours after the last OVA challenge and then used for either (*B*) cell count or (*C*) measurement of cytokine concentrations. Mice treated with saline were used as controls. OVA-treated *Foxf1*$^{+/-}$ mice displayed increased total cell count, elevated eosinophil numbers, and increased concentrations of IL-4 and IL-5 compared with OVA-treated WT mice. Mean ± SD was calculated using five mice in each group. *Asterisks* indicate statistically significant differences with $P < 0.05$. (*D* and *E*) Methacholine-induced airway hyperresponsiveness in *Foxf1*$^{+/-}$ mice. Airway responsiveness was measured 24 h after the last OVA challenge. *Foxf1*$^{+/-}$ mice displayed reduced basal airway resistance (*solid triangles*) compared with WT mice (*solid squares*). OVA challenges increased airway responsiveness to 1.25–2.5 mg/ml of methacholine in *Foxf1*$^{+/-}$ mice (*open triangles*) when compared with OVA-treated WT mice (*open squares*). Rrs ratio between OVA-treated and saline-treated mice was increased in *Foxf1*$^{+/-}$ mice (*E*). (*F*) Increased concentrations of CXCL12 protein in BAL fluid of OVA-treated *Foxf1*$^{+/-}$ mice. BAL fluid was collected from WT or *Foxf1*$^{+/-}$ mice 24 hours after the last OVA challenge. Five mice were used for each group. (*G*) Decreased Foxf1 expression and increased expression of tryptase and CXCL12 in injured *Foxf1*$^{+/-}$ lungs. Total RNA was prepared from left lung lobe of OVA-challenged WT and *Foxf1*$^{+/-}$ mice (4–5 mice in each group) and then used for quantitative real-time RT-PCR with primers specific to mouse Foxf1, CXCL12, tryptase, and cyclophilin. Individual samples were normalized to the corresponding cyclophilin mRNA levels. *Asterisks* indicate statistically significant differences with *P* values < 0.05.

mast cell migration and chemotaxis (4). These results suggest that haploinsufficiency of the *Foxf1* gene increases pulmonary mast cell numbers during embryonic lung development, perhaps through a CXCL12-dependent mechanism. Activation of mast cells causes blood vessel dilatation and inhibits blood coagulation due to release of histamine and heparin, respectively (1, 2). Because a majority of *Foxf1*$^{+/-}$ mice exhibited a perinatal lethal phenotype due to pulmonary hemorrhage (13), it is tempting to speculate that mast cell–derived mediators contribute to the pulmonary hemorrhage seen in newborn *Foxf1*$^{+/-}$ mice (13).

In the present study, we demonstrated an increased susceptibility of *Foxf1*$^{+/-}$ mice to both chemical and allergen-mediated lung inflammation. In studies of CCl_4 toxicity, severe airway obstruction and bronchial edema in *Foxf1*$^{+/-}$ mice preceded the onset of severe hepatic injury (18), suggesting that the liver injury does not cause mortality in *Foxf1*$^{+/-}$ mice. Pulmonary inflammation was associated with elevated tryptase and increased numbers of mast cells. Since degranulation of mast cells is known to cause the release of tryptase and histamine into the airways enhancing inflammation and leading to bronchial edema and bronchoconstriction (31, 32, 35, 36), our results suggest that CCl_4 injury caused degranulation of pulmonary mast cells, contributing to bronchial edema and lethality of the *Foxf1*$^{+/-}$ mice from airway obstruction. Although CCl_4-treated *Foxf1*$^{+/-}$ mice developed respiratory symptoms before death, it is not sufficient to conclude that the lethality occurred solely due to mast cell degranulation and pulmonary inflammation. Liver injury can also contribute, at least in part, to the lethality observed in CCl_4-treated *Foxf1*$^{+/-}$ mice. In fact, abnormal degranulation of mast cells in *Foxf1*$^{+/-}$ lungs may be triggered by systemic release of cytokines, chemokines, and/or enzymes from injured liver. We previously demonstrated that hepatic expression of IFN-β, IFN-γ, TNF-α, and IL-6 were not changed in CCl_4-treated *Foxf1*$^{+/-}$ mice, whereas the *Foxf1*$^{+/-}$ livers produced increased levels of TGF-β1 (18). Since TGF-β1 is a potent chemoattractant for mast cells (6), increased TGF-β1 activity in CCl_4-treated *Foxf1*$^{+/-}$ mice may contribute to abnormal mast cell activation and/or recruitment in the lung. Furthermore, since Foxf1 is highly expressed in peribronchial smooth muscle cells (12, 13), it is also

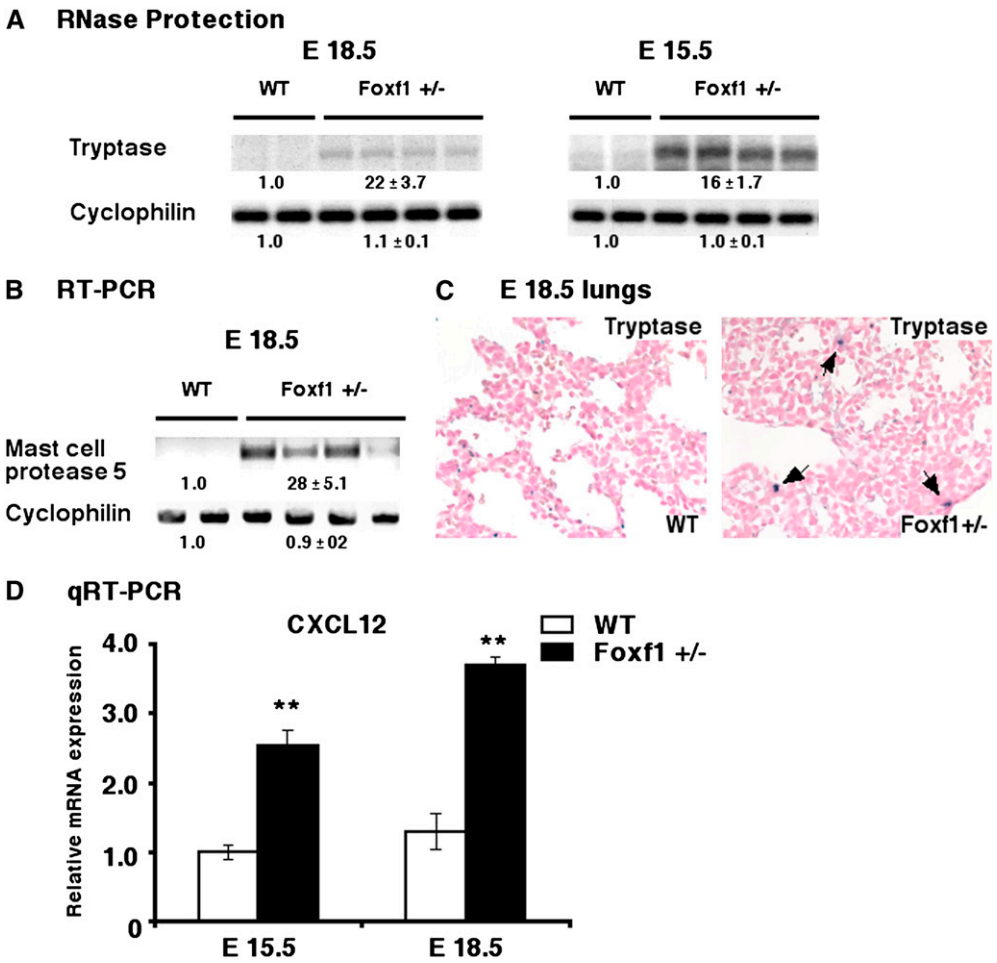

Figure 6. Increased numbers of mast cells and elevated CXCL12 expression in *Foxf1*$^{+/-}$ embryonic lungs. (*A* and *B*) Increased tryptase and mast cell protease-5 mRNAs were detected in fetal lungs of *Foxf1*$^{+/-}$ embryos at E15.5 and E18.5. Total RNA isolated from either *Foxf1*$^{+/-}$ or WT E15.5 and E18.5 lungs was subjected to (*B*) RT-PCR analysis with primers specific to mast cell protease-5 or (*A*) RNase protection assays with probes for mast cell tryptase. Numbers represent fold increase in gene expression (mean ± SD) in *Foxf1*$^{+/-}$ lungs compared with WT lungs. (*C*) Increased numbers of mast cells in lungs of *Foxf1*$^{+/-}$ embryos. Paraffin lung sections from *Foxf1*$^{+/-}$ and WT E18.5 embryos were stained with antibodies against mast cell tryptase to visualize pulmonary mast cells (shown with *arrows*). Lung sections were counterstained with nuclear fast red. Increased numbers of tryptase-positive mast cells were observed in *Foxf1*$^{+/-}$ lungs. *Magnification*: ×200. (*D*). Increased CXCL12 expression in *Foxf1*$^{+/-}$ embryonic lungs. Total RNA was isolated from either E15.5 or E18.5 lungs and then subjected to qRT-PCR analysis with primers specific to CXCL12. Each individual sample was normalized to its corresponding cyclophilin level and presented as a mean ± SD in four different embryos. *Asterisks* indicate statistically significant differences with P values < 0.05 as calculated by Student's t test.

possible that Foxf1 haploinsufficiency influences muscular constriction in *Foxf1*$^{+/-}$ airways, thus contributing to airway obstruction and lethality.

Our previous studies demonstrated that *Foxf1*$^{+/-}$ mice died of pulmonary hemorrhage after BHT lung injury (17). This mortality with *Foxf1*$^{+/-}$ lung injury was associated with a significant reduction in pulmonary Foxf1 levels and diminished expression of genes critical for lung repair (17). In present study, we also found that BHT-treated *Foxf1*$^{+/-}$ lungs displayed elevated numbers of pulmonary mast cells and increased tryptase levels, causing airway obstruction. These results suggest that mast cell degranulation and bronchial edema contributes to the lethality in BHT-treated *Foxf1*$^{+/-}$ mice.

Another important finding of our studies is that *Foxf1*$^{+/-}$ mice displayed increased lung inflammation and airway hyperresponsiveness to methacholine after OVA sensitization and OVA challenge. Increased tryptase levels were also observed in OVA-challenged *Foxf1*$^{+/-}$ lungs, suggesting that antigen-mediated response can trigger mast cell degranulation in *Foxf1*$^{+/-}$ lungs. This may enhance pulmonary inflammation and airway hyperresponsiveness in *Foxf1*$^{+/-}$ lungs. Because increased numbers of mast cells were observed in untreated *Foxf1*$^{+/-}$ lungs, Foxf1 haploinsufficiency may contribute to a genetic predisposition to antigen-mediated lung inflammation and asthma. Interestingly, an increased number of activated mast cells is also characteristic of systemic mastocytosis, a heterogeneous group of human disorders characterized by myeloproliferative syndrome and elevated tryptase levels in multiple organs (8). Since ablation of a single allele of the Foxf1 gene caused increased numbers of mast cells, it will be of interest to assess status of the Foxf1 gene in human mastocytosis.

Although mechanisms underlying increased numbers of mast cells in *Foxf1*$^{+/-}$ lungs remain unclear, our results suggest that Foxf1 is involved in regulation of mast cell homeostasis or migration. The Foxf1 protein is a transcription factor, which is expressed in pulmonary fibroblasts, ECs, and smooth muscle cells, but not in hematopoetic cells (12, 13). Using either Foxf1 antibody or LacZ staining detecting a β-galactosidase reporter knocked into endogenous Foxf1 gene locus (13), we were unable to detect the Foxf1 in mast cells, basophils, or their precursors in the bone marrow or embryonic liver (18, 34, and data not shown). Therefore, Foxf1 regulates mast cell homeostasis or recruitment by an indirect mechanism, possibly involving pulmonary endothelial cells, a major cell type expressing Foxf1 protein in the lung (12, 13).

In the present study, we used an inducible Foxf1 dominant-negative transgene (Foxf1 DN) (29) to inhibit Foxf1 function in primary lung ECs prepared from either WT or TetO-Foxf1 DN transgenic mice. Our results demonstrated that Foxf1 depletion in cultured ECs induces the expression of CXCL12, a chemokine known to promote mast cell migration and chemotaxis (4). Thus, Foxf1 negatively regulates CXCL12 expression in cultured endothelial cells *in vitro*. Consistent with this hypothesis, increased expression of CXCL12 was found in *Foxf1*$^{+/-}$ lungs after either chemically induced (CCl_4 and BHT) or antigen-mediated (OVA) lung injury, correlating with increased number of mast cells and elevated tryptase levels in *Foxf1*$^{+/-}$ lungs. Interestingly, five potential forkhead-binding sites are present in the −2 kb

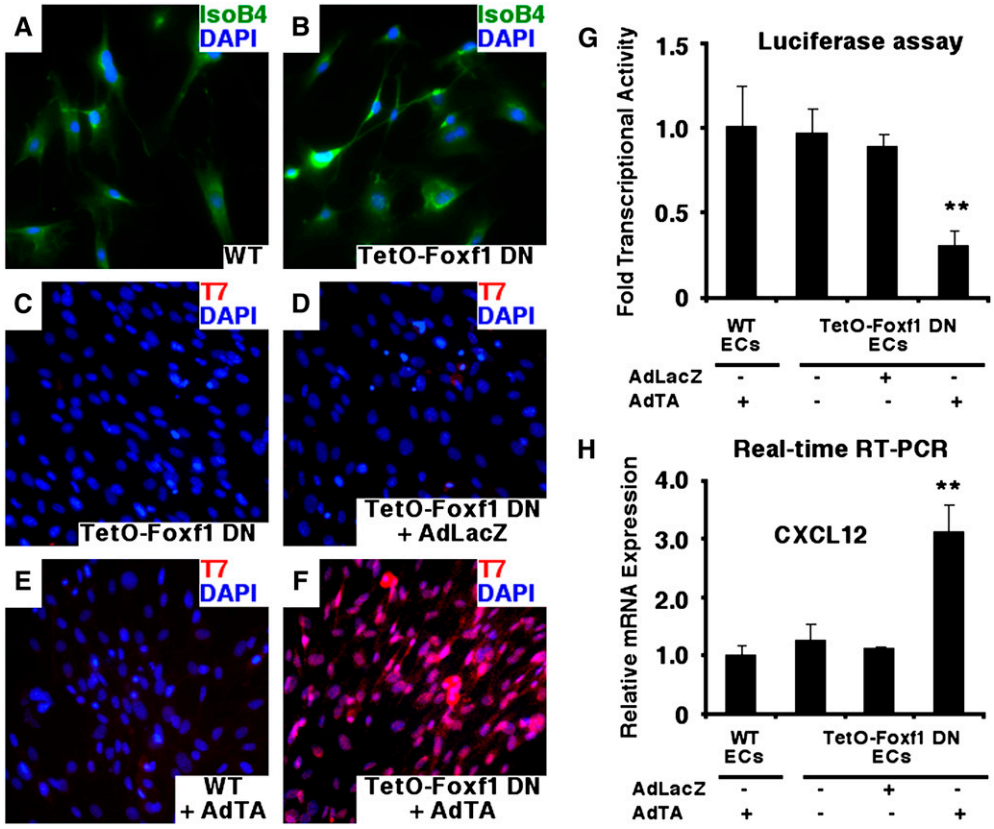

Figure 7. Conditional expression of Foxf1 DN protein in primary endothelial cells induces CXCL12 expression. (*A* and *B*) Purified ECs express endothelial marker isolectin B4. Cultured primary ECs were fixed and stained with FITC-conjugated isolectin B4 (IsoB4, Vector lab, *green staining*) followed by DAPI counterstain (*blue nuclei*) to visualize endothelial cells. (*C–F*) Increased expression of Foxf1 DN protein in transgenic ECs infected with AdTA adenovirus. Transgenic TetO-Foxf1 DN or WT endothelial cells were infected with adenovirus containing Tetracycline activator (AdTA, Tet-off system) or control AdLacZ adenovirus. Cells were then fixed and used for immunofluorescent staining with T7 antibody (*red*) followed by DAPI counterstain (*blue*) to visualize cells expressing the Foxf1 DN transgene. (*G*) Foxf1 transcriptional activity is reduced in transgenic TetO-Foxf1 DN ECs after infection with AdTA. Transgenic or WT ECs were transiently transfected with 6× Foxf1 TATA-luciferase reporter plasmid and CMV-Foxf1 expression vector and then infected with either AdTA or control AdLacZ adenovirus. Cells were harvested 48 hours later and processed for dual luciferase assay to determine luciferase activity. Transcriptional activity is presented as means ± SD. *P* values ≤ 0.05 are identified with *asterisks*. (*H*) CXCL12 expression is induced in transgenic TetO-Foxf1 DN ECs after infection with AdTA. Total RNAs were prepared from transgenic TetO-Foxf1 DN and WT endothelial cells that were infected with either AdTA adenovirus or control AdLacZ adenovirus. CXCL12 expression was determined by qRT-PCR. CXCL12 mRNA levels were normalized to the corresponding cyclophilin levels and presented as a mean ± SD in four different EC cultures.

promoter region of the mouse CXCL12 gene (−936, −1,219, −1,335, −1,419, and −1,807), raising the possibility that Foxf1 may bind to this promoter region and act as a repressor of CXCL12 gene transcription. Alternatively, since a repressor function has not previously been reported for the Foxf1 transcription factor, the Foxf1 protein may indirectly regulate the CXCL12 gene. It is also possible that the absence of Foxf1 allows other transcriptional activators, more potent then Foxf1, to bind the promoter region, thus inducing CXCL12 gene expression.

In summary, *Foxf1*$^{+/-}$ mice displayed severe airway obstruction, elevated numbers of pulmonary mast cells, and increased tryptase levels after various forms of lung injury. Pulmonary inflammation in *Foxf1*$^{+/-}$ mice was associated with diminished expression of Foxf1, and increased expression of CXCL12, the latter of which is essential for mast cell migration and chemotaxis. Increased numbers of mast cells, and elevated CXCL12 levels, were found in lungs of *Foxf1*$^{+/-}$ embryos. Foxf1 depletion in cultured endothelial cells led to a significant increase in CXCL12 expression. Our results suggest that Foxf1 haploinsufficiency causes genetic predisposition to inflammatory lung diseases in mice due, at least in part, to increased recruitment of mast cells to the lung and increased CXCL12 production by pulmonary endothelial cells.

Conflict of Interest Statement: None of the authors has a financial relationship with a commercial entity that has an interest in the subject of this manuscript.

Acknowledgments: The authors thank S. Ramakrishna, D. Malin, and I. M. Kim for technical assistance and Lloyd Graf Jr. for useful comments. The authors dedicate this manuscript to the memory of Robert H. Costa, a pioneer in discovery and characterization of Forkhead transcription factors.

References

1. Metcalfe DD, Baram D, Mekori YA. Mast cells. *Physiol Rev* 1997;77: 1033–1079.
2. Coleman JW. Nitric oxide: a regulator of mast cell activation and mast cell-mediated inflammation. *Clin Exp Immunol* 2002;129:4–10.
3. Gordon JR, Galli SJ. Mast cells as a source of both preformed and immunologically inducible tnf-alpha/cachectin. *Nature* 1990;346:274–276.
4. Lin TJ, Issekutz TB, Marshall JS. Human mast cells transmigrate through human umbilical vein endothelial monolayers and selectively produce il-8 in response to stromal cell-derived factor-1 alpha. *J Immunol* 2000;165:211–220.
5. Gruber BL, Marchese MJ, Kew R. Angiogenic factors stimulate mast-cell migration. *Blood* 1995;86:2488–2493.
6. Gruber BL, Marchese MJ, Kew RR. Transforming growth factor-beta 1 mediates mast cell chemotaxis. *J Immunol* 1994;152:5860–5867.
7. Belot MP, Abdennebi-Najar L, Gaudin F, Lieberherr M, Godot V, Taieb J, Emilie D, Machelon V. Progesterone reduces the migration of mast cells toward the chemokine stromal cell-derived factor-1/cxcl12 with an accompanying decrease in cxcr4 receptors. *Am J Physiol* 2007;292:E1410–E1417.
8. Akin C. Clonality and molecular pathogenesis of mastocytosis. *Acta Haematol* 2005;114:61–69.
9. Kaestner KH, Knochel W, Martinez DE. Unified nomenclature for the winged helix/forkhead transcription factors. *Genes Dev* 2000;14:142–146.
10. Costa RH, Kalinichenko VV, Lim L. Transcription factors in mouse lung development and function. *Am J Physiol Lung Cell Mol Physiol* 2001; 280:L823–L838.
11. Perl AK, Whitsett JA. Molecular mechanisms controlling lung morphogenesis. *Clin Genet* 1999;56:14–27.
12. Kalinichenko VV, Lim L, Shin B, Costa RH. Differential expression of forkhead box transcription factors following butylated hydroxytoluene lung injury. *Am J Physiol Lung Cell Mol Physiol* 2001;280: L695–L704.

13. Kalinichenko VV, Lim L, Beer-Stoltz D, Shin B, Rausa FM, Clark J, Whitsett JA, Watkins SC, Costa RH. Defects in pulmonary vasculature and perinatal lung hemorrhage in mice heterozygous null for the forkhead box f1 transcription factor. *Dev Biol* 2001;235:489–506.
14. Mahlapuu M, Ormestad M, Enerback S, Carlsson P. The forkhead transcription factor foxf1 is required for differentiation of extra-embryonic and lateral plate mesoderm. *Development* 2001;128:155–166.
15. Mahlapuu M, Enerbäck S, Carlsson P. Haploinsufficiency of the forkhead gene foxf1, a target for sonic hedgehog signaling, causes lung and foregut malformations. *Development* 2001;128:2397–2406.
16. Lim L, Kalinichenko VV, Whitsett JA, Costa RH. Fusion of right lung lobes and pulmonary vessels in mice heterozygous for the forkhead box f1 targeted allele. *Am J Physiol Lung Cell Mol Physiol* 2002;282: L1012–L1022.
17. Kalinichenko VV, Zhou Y, Shin B, Beer-Stoltz D, Watkins SC, Whitsett JA, Costa RH. Wild type levels of the mouse forkhead box f1 gene are essential for lung repair. *Am J Physiol Lung Cell Mol Physiol* 2002;282:L1253–L1265.
18. Kalinichenko VV, Bhattacharyya D, Zhou Y, Gusarova GA, Kim W, Shin B, Costa RH. Foxf1 +/− mice exhibit defective stellate cell activation and abnormal liver regeneration following ccl4 injury. *Hepatology* 2003;37:107–117.
19. Kim IM, Zhou Y, Ramakrishna S, Hughes DE, Solway J, Costa RH, Kalinichenko VV. Functional characterization of evolutionary conserved DNA regions in forkhead box f1 gene locus. *J Biol Chem* 2005; 280:37908–37916.
20. Wang X, Hung N-J, Costa RH. Earlier expression of the transcription factor hfh 11b (foxm1b) diminishes induction of p21$^{cip1/waf1}$ levels and accelerates mouse hepatocyte entry into s-phase following carbon tetrachloride liver injury. *Hepatology* 2001;33:1404–1414.
21. Kalinichenko VV, Gusarova GA, Tan Y, Wang IC, Major ML, Wang X, Yoder HM, Costa RH. Ubiquitous expression of the forkhead box m1b transgene accelerates proliferation of distinct pulmonary cell-types following lung injury. *J Biol Chem* 2003;278:37888–37894.
22. Myou S, Leff AR, Myo S, Boetticher E, Tong J, Meliton AY, Liu J, Munoz NM, Zhu X. Blockade of inflammation and airway hyperresponsiveness in immune-sensitized mice by dominant-negative phosphoinositide 3-kinase-tat. *J Exp Med* 2003;198:1573–1582.
23. Kalinichenko VV, Mokyr MB, Graf LH Jr, Cohen RL, Chambers DA. Norepinephrine-mediated inhibition of antitumor cytotoxic t lymphocyte generation involves a beta-adrenergic receptor mechanism and-decreased tnf-alpha gene expression. *J Immunol* 1999;163:2492–2499.
24. Wang X, Quail E, Hung N-J, Tan Y, Ye H, Costa RH. Increased levels of forkhead box m1b transcription factor in transgenic mouse hepatocytes prevents age-related proliferation defects in regenerating liver. *Proc Natl Acad Sci USA* 2001;98:11468–11473.
25. Kalinichenko VV, Zhou Y, Bhattacharyya D, Kim W, Shin B, Bambal K, Costa RH. Haploinsufficiency of the mouse forkhead box f1 gene causes defects in gall bladder development. *J Biol Chem* 2002;277: 12369–12374.
26. Kim IM, Ackerson T, Ramakrishna S, Tretiakova M, Wang IC, Kalin TV, Major ML, Gusarova GA, Yoder HM, Costa RH, *et al.* The forkhead box m1 transcription factor stimulates the proliferation of tumor cells during development of lung cancer. *Cancer Res* 2006;66: 2153–2161.
27. Zhao YY, Gao XP, Zhao YD, Mirza MK, Frey RS, Kalinichenko VV, Wang IC, Costa RH, Malik AB. Endothelial cell-restricted disruption of foxm1 impairs endothelial repair following lps-induced vascular injury. *J Clin Invest* 2006;116:2333–2343.
28. Frey RS, Rahman A, Kefer JC, Minshall RD, Malik AB. Pkczeta regulates tnf-alpha-induced activation of nadph oxidase in endothelial cells. *Circ Res* 2002;90:1012–1019.
29. Malin D, Kim IM, Boetticher E, Kalin TV, Ramakrishna S, Meliton L, Ustiyan V, Zhu X, Kalinichenko VV. Forkhead box f1 is essential for migration of mesenchymal cells and directly induces integrin-beta3 expression. *Mol Cell Biol* 2007;27:2486–2498.
30. Kim IM, Ramakrishna S, Gusarova GA, Yoder HM, Costa RH, Kalinichenko VV. The forkhead box m1 transcription factor is essential for embryonic development of pulmonary vasculature. *J Biol Chem* 2005;280:22278–22286.
31. Swystun VA, Gordon JR, Davis EB, Zhang X, Cockcroft DW. Mast cell tryptase release and asthmatic responses to allergen increase with regular use of salbutamol. *J Allergy Clin Immunol* 2000;106:57–64.
32. Oh SW, Pae CI, Lee DK, Jones F, Chiang GK, Kim HO, Moon SH, Cao B, Ogbu C, Jeong KW, *et al.* Tryptase inhibition blocks airway inflammation in a mouse asthma model. *J Immunol* 2002;168:1992–2000.
33. Walls AF, Jones DB, Williams JH, Church MK, Holgate ST. Immunohistochemical identification of mast cells in formaldehyde-fixed tissue using monoclonal antibodies specific for tryptase. *J Pathol* 1990;162: 119–126.
34. Kalinichenko VV, Gusarova GA, Shin B, Costa R. The forkhead box f1 transcription factor is expressed in brain and head mesenchyme during mouse embryonic development. *Gene Expr Patterns* 2003;3: 153–158.
35. Hart PH. Regulation of the inflammatory response in asthma by mast cell products. *Immunol Cell Biol* 2001;79:149–153.
36. Wright CD, Havill AM, Middleton SC, Kashem MA, Dripps DJ, Abraham WM, Thomson DS, Burgess LE. Inhibition of allergen-induced pulmonary responses by the selective tryptase inhibitor 1,5-bis-[4-[(3-carbamimidoyl-benzenesulfonylamino)-methyl]-phenoxy]-pen tane (amg-126737). *Biochem Pharmacol* 1999;58:1989–1996.